β-cyclodextrin functionalized graphene as a highly conductive and multi-site platform for DNA immobilization and ultrasensitive sensing detection

Yizhen Yang, Feng Gao, Xili Cai, Xiaoning Yuan, Suyu He, Fei Gao, Hongxu Guo, Qingxiang Wang

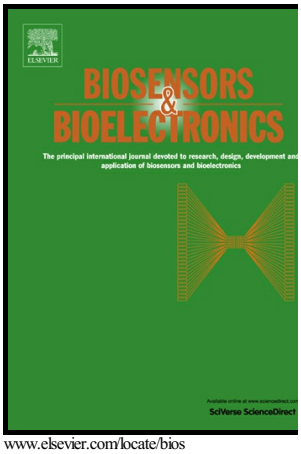

www.elsevier.com/locate/bios

PII: S0956-5663(15)30186-X
DOI: http://dx.doi.org/10.1016/j.bios.2015.06.018
Reference: BIOS7754

To appear in: *Biosensors and Bioelectronic*

Received date: 1 April 2015
Revised date: 26 May 2015
Accepted date: 9 June 2015

Cite this article as: Yizhen Yang, Feng Gao, Xili Cai, Xiaoning Yuan, Suyu He, Fei Gao, Hongxu Guo and Qingxiang Wang, β-cyclodextrin functionalized graphene as a highly conductive and multi-site platform for DNA immobilization and ultrasensitive sensing detection, *Biosensors and Bioelectronic* http://dx.doi.org/10.1016/j.bios.2015.06.018

β-cyclodextrin functionalized graphene as a highly conductive and multi-site platform for DNA immobilization and ultrasensitive sensing detection

Yizhen Yang, Feng Gao*, Xili Cai, Xiaoning Yuan, Suyu He, Fei Gao, Hongxu Guo, Qingxiang Wang*

College of Chemistry and Environment, Fujian Province Key Laboratory of Morden Analytical Science and Separation Technology, Minnan Normal University, Zhangzhou 363000, P. R. China

Submitted to **Biosensors and Bioelectronics**

**Authors for correspondence*

Ph.D. Feng Gao

Tel: +86-596-2591445;

Fax: +86-596-2520035;

E-mail:Fgao1981@126.com.

Prof. Qingxiang Wang

Tel: +86-596-2596780;

Fax: +86-596-2527801;

E-mail: axiang236@126.com.

Abstract

A versatile nanocomposite containing β-cyclodextrin and graphene (CD-GR) was prepared through a simple chemical reduction method. The characterization experiments show that the nanocomposite remains the flake-like morphology of GR, but its solubility and stability in aqueous solution are greatly improved. Then the nanocomposite was modified at glassy carbon electrode (GCE) surface, and was used as a functional matrix for the covalent immobilization of probe DNA using 2,4,6-trichloro-1,3,5-triazine (TCT) as the crosslinker. Due to the synergetic effect of large surface area of GR and rich hydroxyl of CD, the probe density for the developed biosensor was determined to as high as 3.82×10^{13} molecules cm^{-2}. Meanwhile, the biosensor shows high hybridization efficiency and hybridization kinetic. When the

biosensor was applied for the impedance-based hybridization test, a wide linear range from 1.0×10^{-16} to 1.0×10^{-12} M and an ultralow detection limit of 3.4×10^{-17} M were achieved. The biosensor also displays excellent stability, selectivity, and reproducibility.

Keywords

Graphene;
β-cyclodextrin;
2,4,6-trichloro-1,3,5-triazine;
DNA biosensor.

1. Introduction

In the past two decades, there has been a considerable growth of interest in sequence-specific DNA detection due to its significant potential in the application of gene analysis, clinical diagnosis, drug screening, forensic and environmental identification, and food safety monitoring (Li et al. 2008; Xu et al. 2009; Vickery et al. 2009). However, the DNA amounts extracted from physiological and other biological samples are often low to femtomolar (fM) or even attomolar (aM), which is much lower than the detection limits of most conventional techniques (Xia et al. 2015). The polymerase chain reaction (PCR) technology can effectively improve the sensitivity of DNA detection by amplificating DNA samples. Nonetheless, the procedure is cumbersome, expensive, time-consuming, and the range of target DNA quantification is narrow after amplification (Cui et al. 2015).

Alternatively, the electrochemical method that mainly based on the electrochemical DNA biosensors has been widely used for DNA analysis due to its small dimensions, 1ow cost and good compatibility with microfabrication technology (Du et al. 2010; Wang et al. 2009). In order to improve the analytical performance of the electrochemical DNA biosensors, many new strategies such as nanoparticles labeling (Rai et al. 2012), molecule beacons (Chen et al. 2013), enzyme-assisted target recycling (Wang et al. 2013) have been introduced into the construction of DNA biosensors. Although these methods are effective, the development of appropriate methods to immobilize probe DNA on a transducer surface is still a basic and critical task for the construction of a high-powered DNA biosensor, because many properties such as sensitivity, hybridization efficiency, as well as the stability and regeneration

ability can be well controlled by the probe immobilization effect.

Based on this, nanomaterials receive increasing interest in electrochemical DNA biosensor fabrication as matrixes, due to their versatile properties such as large surface area, high electrocatalytic capacity, and excellent chemical and physical stability (Zhang et al. 2008). Graphene (GR), a two-dimensional sheet-like material constituted by sp^2-bonded carbon atoms, attracts widespread attention in various fields such as nanoelectronics (Qin et al. 2014), nanophotonics (Yu et al. 2014), nanocomposites (Eck et al. 2014), and sensors (Feng et al. 2014). Recently, its application in electrochemistry has been highlighted due to its high mechanical strength, large surface area, non-toxicity and rapid heterogeneous electron transfer ability (Peng et al. 2015; Deng et al. 2013). However, the single-component GR is easy to form irreversible agglomerates or even restack to form graphite through strong π-π stacking or van der waals interaction, which limited its practical application in electrochemical field. In contrast, many functionalized GR nanocomposites not only avoid the disadvantages of single GR, but also combine the advantages of both GR and the modifiers. Therefore, large amounts of GR-based nanocomposites are designed and synthesized, and used as electrode materials (Deng et al. 2013; Wang et al. 2014).

β-cyclodextrin (CD) is a cyclic oligosaccharide consisting of seven glucose. It is toroidal in shape with a hydrophobic inner cavity and a hydrophilic outer surface (Freeman et al. 2009). It has been reported that the CD can be adsorbed on the surface of GR through the strong hydrogen bonding, producing a nanocomposite (CD-GR) with good water-solubility. Additionally, the product combines the unique properties of GR (large surface area and high conductivity) and CD (high supramolecular recognition ability). Based on this, CD-GR has been applied as the electrode material for the specific and sensitive electrochemical detection of many small molecules including isoquercitrin (Liu et al. 2014), baicalin (Liu et al. 2014), chlorophenol (Wei et al. 2014), and quercetin (Zhang et al. 2014), *ect*.

However, all these sensors are based on host-guest recognition of analytes and CD, and to the best of our knowledge, the CD-GR has also not been used as an immobilization matrix for bioprobe molecules. In this work, inspired by feature of large surface area, high conductivity and rich active hydroxy groups of CD in the composite of CD-GR, a new DNA biosensor was fabricated by grafting the probe DNA fragments on the surface of CD-GR modified electrode, using a highly chemical

active 2,4,6-trichloro-1,3,5-triazine (TCT) as the crosslinker (Fig. 1). The results show that due to the large surface area and rich hydroxy groups of the composite, the loading density of probe DNA on the electrode surface was determined to be as high as 3.82×10^{13} molecules cm^{-2}. When the electrochemical impedance technology was applied for the hybridization detection, low background response, fast hybridization rate and high hybridization efficiency were obtained. The target DNA can be detected by the developed biosensor over a wide linear range from 1.0×10^{-16} to 1.0×10^{-12} M, with an ultralow detection limit of 3.4×10^{-17} M, which greatly broadens the application of this category of materials in the electrochemical field.

<Fig. 1 >

2. Experimental

2.1 Reagents and apparatus

β-Cyclodextrin (CD) was provided by Sinopharm Chemical Reagent Co., Ltd. (Shanghai, China). 2,4,6-trichloro-1,3,5-triazine (TCT) and Hexammineruthenium (III) chloride (RuHex) were purchased from Sigma-Aldrich Co., Ltd. (Shanghai, China). Tris(hybroxymethyl) aminomethane (Tris) was obtained from Aladdin Reagent Co., Ltd. (Shanhai, China). Ethylenediaminetetraacetic acid (EDTA) was purchased from Xilong Chemical Co., Ltd (Guandong, China). GO was synthesized through according to Hummer's method with minor modification, and the detailed procedure is given in Supporting Information. All the chemicals were of analytical reagent grade and used without further purification. The doubly distilled water (DDW) was used throughout this work.

The 18-base DNA sequences were synthesized by Shanghai Sangon Bioengineering Co., Ltd. (Shanghai, China). Their base sequences are as follows:

- Probe sequence (S1): 5'-NH_2-$(CH_2)_6$-TCT TTG GGA CCA CTG TCG-3'
- Complementary sequence (S2): 5'-CGA CAG TGG TCC CAA AGA-3'
- One-base mismatched sequence (S3): 5'-CGA CAG TGG TCC CAA *C*GA-3'
- Three-base mismatched sequence (S4): 5'-CGA CA*A* TGG *C*CC CAA *C*GA-3'
- Non-complementary sequence (S5): 5'-GCA TCG AGC GAG CAC GTA-3'

Stock solution (10 μM) of all oligonucleotides were prepared with TE buffer solution (10 mM Tris-HCl, 1.0 mM EDTA, pH 8.0) and kept at freezing temperatures before use.

The morphology of the prepared CD-GR was characterized on a S-4800 scanning

electron microscope (SEM, Hitachi, Japan) and a Tecnai G2 F20 U-TWIN transmission electron microscope (TEM, FEI, USA). Fourier transform infrared (FT-IR) spectroscopy was recorded on an FT-IR spectrophotometer (Nicolet iS 10, USA). The Raman spectroscopy was conducted on a InVia Raman microscope (Renishaw, USA). The electrochemical measurements including cyclic voltammetry (CV), electrochemical impedance spectroscopy (EIS) and chronocoulometry (CC) were performed using an electrochemical station (CHI 650D, China). A three-electrode system was employed with Pt wire as the auxiliary electrode, an Ag/AgCl (3 M KCl) as the reference electrode and a bare or modified glassy carbon electrode (GCE) as working electrode.

2.2 Preparation of CD functionalized GR (CD-GR) composite

The synthesis of CD functionalized chemical reduced graphene (CD-GR) was carried out according to the following procedures (Guo et al. 2010): 60 mL portion of the homogeneous GO dispersion (0.5 mg mL^{-1}) was mixed with 60 mL of 35 mM CD aqueous solution and 1 mL of ammonia solution (25-28%), followed by the addition of 0.5 mL of hydrazine solution (50%). After vigorous stirring for a few minutes, the vial was heated in a water bath (60 °C) for 8 h, through which the black and stable dispersion was obtained. The dispersion was then filtered through a cellulose acetate membrane (0.22 μm pore size), and washed with DDW for 5 times. After dried by vacuum at room temperature, the CD functionalized graphene (CD-GR) nanocomposite was achieved. The GR counterpart was prepared by the similar route just without the addition of CD during above synthesis process.

2.3 Fabrication of the DNA biosensor

The DNA biosensor was fabricated through the following procedures: Firstly, a GCE was sequentially polished with 0.3 μm and 0.05 μm alumina slurries, and then consecutively ultrasonicated for 5 min in acetone, ethanol, and DDW to remove any contaminants adsorbed on the electrode surface. After dried under N_2 stream, 10 μL 0.5 mg mL^{-1} CD-GR suspension was cast on the surface of the cleaned GCE and dried naturally to obtain CD-GR modified GCE (CD-GR/GCE). Secondly, the CD-GR/GCE was immersed into 1 mL absolute ethanol containing 10 mM TCT for 6 h under 4 °C to undergo the condensation reaction between hydroxyl groups in CD and chlorohydrocarbon in TCT. After rinsing with DDW and dried under N_2

atmosphere, the TCT modified electrode (TCT/CD-GR/GCE) was obtained. Thirdly, the TCT/CD-GR/GCE was incubated in 0.1 μM amino modified probe DNA (S1) solution for 8 h under 40 °C to immobilize S1 via nucleophilic substitution reaction of amino group with residual chlorine group of TCT. After rinsing with PBS to remove physically absorbed DNA, a DNA biosensor (S1/TCT/CD-GR/GCE) was obtained.

2.4 Electrochemical characterization and hybridization detection of the biosensor

The hybridization processes of the developed DNA biosensor were performed by immersing S1/TCT/CD-GR/GCE into 200 μL hybridization solution (TE) containing complementary sequence (S2), one-base mismatched sequence (S3), three-base mismatched sequence (S4) or non-complementary sequence (S5) with the desired concentration for 30 min at 40 °C, and then rinsed with PBS to remove the non-specifically adsorbed DNA. The obtained electrodes were denoted as S2-S1/TCT/CD-GR/GCE, S3-S1/TCT/CD-GR/GCE, S4-S1/TCT/CD-GR/GCE, or S5-S1/TCT/CD-GR/GCE, respectively.

The electrochemical methods including CV and EIS were applied to characterize the stepwise modification of the electrodes. The following parameters were employed for CV: scan rate, 100 mV s^{-1}; potential scanning range, +0.6 V to -0.2 V. The EIS was collected at a potential of +0.2 V in the frequency range of 0.01-10^4 Hz with the voltage amplitude of 5 mV. The supporting electrolyte was 1.0 mM $[Fe(CN)_6]^{3-/4-}$(1:1) with 0.1 M KCl. The hybridization ability of the biosensor was also monitored by EIS under the same conditions mentioned above.

3. Results and discussion

3.1 Structure and morphology characterization of CD-GR nanocomposite

Fig. 2A shows the electronic photographs of GO (a), GR (b) and CD-GR composite (c) dissolved in water. As well seen, a homogenous brown solution was observed for GO, suggesting its good water-solubility in water. When the chemically reduced GR was dispersed in water, some black precipitates were formed within 1 h, which could be explained by the serious aggregation between bare GR sheets through π-π stacking and/or Van der Waals force (Cui et al. 2012). However, a homogeneous black solution was observed for the dispersion of CD-GR, illustrating good dispersibility of CD-GR composite in water. Additionally, no precipitate was observed after the dispersion was stored for more than 2 months, showing that the CD-GR

dispersion also has excellent stability. The reason may lies in the fact that the π-π stacking and Van der Waals force to cause the aggregation between GR nanosheets are effectively prevented by the surface assembled CD molecules. Through such a comparison, it could be concluded that the stability and dispersion of GR could be greatly improved by introducing the polymolecularity of CD onto its surface. The TEM image (Fig. 2B) of CD-GR shows that the composite has the typical flake-like shape and the wrinkle region as the reported single GR (Lu et al. 2013). This result illustrates that the composite of CD-GR maintains the basic structure of GR nanosheet.

<Fig. 2 >

Raman spectroscopy is a powerful non-destructive tool to characterize carbonaceous materials, particularly for distinguishing ordered and disordered crystal structures of carbon. . **Fig.** 2C shows the typical Raman spectra of GO (a), GR (b) and CD-GR (c). As seen, all the three samples have two characteristic peaks, namely, the G band at 1597 cm^{-1} assigning to the E_{2g} phonon of C sp^2 atoms and the D band at 1335 cm^{-1} corresponding to the breathing mode of κ-point phonons of A_{1g} symmetry (Guo et al. 2010). The intensity ratio of the D to G band (I_D/I_G) is generally accepted to reflect the graphitization degree of carbonaceous materials. Through comparison, it could be found that the I_D/I_G value of CD-GR composite (=1.22) was obviously larger than that of GO (=0.97), but comparable to GR (=1.30), suggesting that the reduced state of GR had been formed in the nanocomposite of CD-GR. .

In order to further probe the binding mechanism between CD and GR, the CD-GR composite was further characterized by FT-IR, and the results are displayed in Fig. 2D. It is found that the GR is essentially featureless except the weak C=C conjugation at 1550 cm^{-1} and C-C vibration at 1190 cm^{-1}, suggesting that the GO had been successfully reduced to the GR (Ye et al. 2013). The spectrum of CD presents clear adsorption bands at 2923 cm^{-1}, 1412 cm^{-1}, 1049 cm^{-1} and 881 cm^{-1}, which can be assigned to -CH_2- stretching vibration, C-H/O-H bending vibration, C-C stretching vibration, and ring vibration, respectively. All these bands also can be observed for the synthesized complex of CD-GR, suggesting that the main functional groups on CD are still remained after assembly with GR. However, it is noted that the stretching vibrations of -OH at 3362 cm^{-1} for CD is shifted to 3435 cm^{-1} in the spectrum of CD-GR. Such a typical red-shift suggests that the hydrogen bonding has been formed

between CD and the residual oxygen-containing groups of GR (Guo et al. 2010). Moreover, it is found that the observed peak at 1160 cm^{-1} for CD is absolutely disappeared on the spectrum of CD-GR, which can be explained by the chemical coupling of the hydroxyl groups on the secondary face of CD with the negative oxygen ions through a nucleophilic reaction in synthesis process (Yang et al. 2006).

3.2 Electrochemical characterization of CD-GR

The electrochemical behaviors of the synthesized CD-GR nanocomposite were characterized by CV and EIS in 1.0 mM $[Fe(CN)_6]^{3-/4-}$ (1:1) containing 0.1 M KCl, and the results are showed in Fig. 3. It can be found that a pair of well-defined redox peaks is obtained on the bare GCE (curve a), suggesting that the cleaned GCE behaved as a good basal electrode for electrochemical measurements. For GR/GCE, a pair of clear redox peaks with large background current is observed (curve c), indicating that the GR has great influence on improving of the effective surface area and electron transfer kinetic of the electrode. However, when GCE was modified with single CD, it is observed that the redox peak currents of $[Fe(CN)_6]^{3-/4-}$ decreased dramatically and the peak-to-peak separation (ΔE_p) increased greatly (curve b). This indicates that the electrochemical reaction process of the electroactive $[Fe(CN)_6]^{3-/4-}$ ions on the electrode surface is inhibited by the non-conductive CD film. When the synthesized CD-GR nanocomposite was casted on the GCE surface, the redox peaks of $[Fe(CN)_6]^{3-/4-}$ increased significantly, and the ΔE_p decreased obviously (curve d) in comparison with CD/GCE. This demonstrates that the hybrid material of CD-GR has significant signal amplification effect in electrochemical measurement as compared with CD/GCE, which can be ascribed to fast electron transfer ability of GR in the composite. This also suggests that the non-conductive GO has been successfully reduced to GR in the composite during the chemical reduction process.

The electrochemical behavior of modified electrode was also characterized by EIS, which has been known as a sensitive technology to monitor the electron transfer process at the interface. Fig. 3B presents the typical Nyquist diagrams of different modified electrodes in 1.0 mM $[Fe(CN)_6]^{3-/4-}$ with 0.1 M KCl. The data are fitted by an equivalent circuit as showed in inset of Fig. 3B, where R_s is solution resistance, R_{ct} the charge transfer resistance associated with counter-ions transfer at the film/electrolyte interface, Q_{dl} a constant phase element corresponding to the double-layer capacitance, W the Warburg impedance relating to mass transfer, and C

the capacitance attributing to the film/electrolyte interface. The fitting results (solid lines) are in a good agreement with the real experimental data (dotted curves), and the fitting results of the equivalent circuit model are listed in Table 1 in Supporting Information. As we can see from the table, when CD was modified onto the GCE, R_{et} value was increased from 17.68 Ω to 1492 Ω, suggesting that CD film decrease the interfacial electron transfer kinetic as an insulating layer (curve b). On GR/GCE, a relatively small R_{et} value of 2.77 Ω is observed (curve c), suggesting that the film of GR promotes the electrode transfer process on the electrode surface by its superior conductivity. After CD-GR was modified on the surface of GCE (curve d), the R_{et} value decreases to 200 Ω, proving that CD-GR accelerates the electron transfer between the electrochemical probe of $[Fe(CN)_6]^{3-/4-}$ and the GCE, due to the high electrical conductivity of GR in the composite film. Also, it is found that the capacitance on CD-GR/GCE has about twice as large as that on CD/GCE, suggesting that CD-GR/GCE has the larger accessible surface area than CD/GCE. According to the following equation (Chen et al. 2015):

$$R_{ct} = \left(\frac{RT}{n^2F^2k^0}\right)\left(\frac{1}{C_O^{(1-\alpha)}C_R^{\alpha}}\right) \quad (1)$$

where α (0.5) is the electron transfer coefficient, F (96485 C mol^{-1}) Faraday's constant, C_O and C_R (1.0 mM) the concentrations of $Fe(CN)_6^{3-/4-}$, and A (0.07 cm^2) the geometric area of electrode, the standard heterogeneous electron transfer constant (k^0) on CD/GC and CD-GR/GCE were calculated to be 0.18 and 1.35 s^{-1}, respectively. Therefore, both CV and EIS experiments confirmed the CD-GR nanocomposite can be used as a better electrochemical platform for bioprobe immobilization than the single CD, due to its higher surface area and more excellent electronic conductivity.

It is noteworthy that although the bare GCE and GR/GCE had the lower impedance values than CD-GR/GCE, both of them have not functional groups as CD-GR/GCE, which limited their application as a bioprobe immbolization platform for biosensor construction. Therefore, in the following studies, the CD-GR/GCE with high conductivity and rich active groups was utilized for potential electrochemical sensing application.

<Fig. 3 >

3.3 DNA grafting using TCT as the crosslinker and the hybridization efficiency

Based on the synergistic effect of large surface area from GR and rich functional

groups from CD of the hybrid film, the CD-GR modified GCE was used as a functional platform for DNA immobilization using TCT as the crosslinker. TCT is an important intermediate in the organic synthesis (Whitaker et al. 1991). One of its most important properties is that the TCT can react with amino and/or hydroxyl groups progressively via tuning the reaction temperature (Zhang et al. 2000). Based on this feature, the TCT was also used as a crosslinker to graft the amino modified DNA probe to the hydroxyl groups contained surface of CD-GR in this work. Fig. S-1(A) in Supporting Information shows the CVs response of $[Fe(CN)_6]^{3-/4-}$ towards the stepwise assembly process of TCT and probe DNA on CD-GR/GCE. It is found that after CD-GR/GCE was immersed in TCT solution for 6 h at 4 °C, the redox peaks of $[Fe(CN)_6]^{3-/4-}$ increase to some extent with the decrease of the ΔE_p. This suggests that TCT has been successfully attached on the surface of CD-GR/GCE, and the conjugated π electrons in the triazine ring of TCT make $[Fe(CN)_6]^{3-/4-}$ more easier to communicate electrons with the electrode surface. Then, when TCT/CD-GR/GCE was further reacted with the amino modified DNA under 40 °C, it is found that the redox peaks of $[Fe(CN)_6]^{3-/4-}$ decrease significantly, with the increase of ΔE_p. This is because the negatively charged phosphate backbone on the confined DNA prevents the approaching of $[Fe(CN)_6]^{3-/4-}$ ions to the electrode surface. In the corresponding Nyquist plots as showed in Fig. S-1(B) in Supporting Information, the electron transfer resistance (R_{et}) decrease upon the grafting of TCT and then increase after immobilization of probe DNA. These results clearly confirm that a DNA biosensor has been fabricated using TCT as the crosslinker and CD-GR as the matrix.

The nanocomposite of CD-GR synthesized in this work is consisted of GR with large surface area and CD owning plenty of active hydroxyl groups, which is expected to make the material having the capacity to covalently immobilize large amount of probe molecules in a biosensor fabrication. In order to prove this, the probe density of the DNA biosensor was determined through typical CC method using RuHex as the electrochemical probe (Shi et al. 2013). The detailed principle and equations are displayed in Supporting Information. Fig. 4 shows the CCs of S1/TCT/CD-GR/GCE in 10 mM pH 8.0 Tris-HCl without (a) and with 50 μM RuHex (b). From the intercept of the two CC curves, the charge difference (ΔQ) was determined to be 1.1 μC. Then according to the equations (1)-(2) as displayed in Supporting Information, the surface density (Γ_{DNA}) on the biosensing interface was calculated to be 3.82×10^{13} strands cm^{-2}, which was about 10-fold larger than that of DNA self-assembly monolayer electrode

(Keighley et al. 2008), testifying that the CD-GR nanocomposite plays an important role to improve the loading amount of the probe DNA. What is more, when the biosensor was hybridized with excess amount of target DNA (S2), and then measured in RuHex solution by CC, the ΔQ was determined to be 2.08 μC, corresponding to the DNA density of 7.18×10^{13} molecules cm^{-2}, from which a hybridization efficiency of 88% was achieved for the developed biosensor. It is noticeable that this hybridization efficiency is obviously higher than those obtained at the bare electrode-based with similar probe density (Zhang et al. 2006). This can be explained by the fact that the probe DNA immobilized with the aid of crosslinker of TCT rather than directly at the electrode surface has the higher freedom and flexibility, which is benefit for the probe strands to sufficiently react with the target DNA. In addition, due to the surface area effect of the nanosized CD-GR, the probe strands on the sensing interface have the larger space to accommodate the target DNA for hybridization.

<Fig. 4 >

3.4 Analytical performance of the DNA biosensor

In order to obtain the optimal analytical performance of the DNA biosensor, some conditions for fabricating the DNA biosensor and hybridization detection were optimized, and the results are displayed in Supporting Information. Under the optimal hybridization condition, the sensitivity of the biosensor was investigated by hybridization with various concentrations of complementary DNA (S2). Fig. 5A shows the typical Nyquist plots of the biosensor upon hybridization with the increasing amounts of target DNA. It is found that the R_{et} values show a gradual increase with the increase of S2 concentrations (C_{S2}) in the hybridization solution. The difference values (ΔR_{et}) between R_{et} at probe DNA modified electrode and those at different hybridized electrodes are found to be well proportional to the logarithm of C_{S2} (lg C_{S2}) in the range from 1.0×10^{-16} M to 1.0×10^{-12} M with a linear equation of $\Delta R_{et}/10^3$ Ω=1.8067 lg (C_{S2}/M)＋29.8651, γ=0.9973. The detection limit of 3.4×10^{-17} M at a signal-to-noise ratio of 3σ (where σ is the standard deviation of a blank solution, n=7) was obtained. The sample volum used in this measurement is 200 μL, therefore the absolute detection limit of the biosensor to target DNA is equivalent to 4.1×10^3 molecules, which suggests that the developed biosensor is much appropriate for practical detection of DNA in physiological levels. Table 2 in Supporting

Information lists the comparison of the detection limits and linear ranges of different GR-based DNA biosensors. Through comparison, it can be found that the fabricated biosensor with high probe density and hybridization efficiency shows a much lower limit of detection than the others, suggesting that our DNA biosensor exhibits an outstanding sensitivity.

The hybridization selectivity of the developed biosensor was further investigated through hybridization with various DNA sequences. Fig. 5C shows the obtained Nyquist diagrams of S1/TCT/CD-GR/GCE upon hybridization with different sequences. It is clear that the value of R_{et} on S5 hybridized electrode (curve b) is very close to that on probe electrode (curve a), suggesting that the states of these two electrodes are similar. This also means that S5 has not been captured to the surface of S1/TCT/CD-GR/GCE due to the full base-mismatching. While, the obtained R_{et} value increases extremely after the biosensor was hybridized with fully complementary sequences (curve e), which can be explained that more negative charges are formed on the electrode surface due to the formation of the intact duplex between S1 and the complementary S2. Moreover, the high selectivity of the biosensor was assessed by detecting the analytes sequences with the different base-mismatch number. It is found that as compared with the case of fully complementary sequences, obviously reduced R_{et} values (6.3 KΩ and 7.8 KΩ) are observed when three-base and one-base mismatched target sequences were hybridized (curve c and curve d, respectively), and meanwhile the R_{et} values increases with the decrease of the base number of mismatch, further suggesting that the developed biosensor has the ability to recognize the target sequences with the different complementary degree.

<Fig. 5 >

3.5 Reproductivity, regeneration and stability of the biosensor

The reproductivity, regeneration and stability are important properties of a DNA biosensor. In this work, the reproductivity of the biosensor was monitored by using five parallel-made DNA biosensors to detect 1.0×10^{-12} M target DNA, and the results shows that a relative standard deviation (RSD) of 2.8% (n=5) was estimated, showing a high reproductibility of the constructed DNA biosensor. Regeneration of the biosensor was performed by thermal denaturation in 90 °C water for 10 min, and the result showed that the developed biosensor could be repeatedly used for hybridization-denaturation-hybridization circles for 10 times, and only a decrease of

5.8% in R_{et} response was obtained. Store of S1/TCT/CD-GR/GCE at 4 ℃ for 7 days resulted in a change of 4.2% in the initial R_{et} response, suggesting a good stability of the biosensor.

4. Conclusions

In this paper, a water-soluble, stable and robust CD-GR nanocomposite was prepared through a simple chemical reduction method. The synthesized nanocomposite shows good homogeneity, dispersibility and stability in aqueous solution, and remains the morphology of graphene. The nanocomposite, for the first time, was used as a highly conductive and multi-site matrix for probe DNA immobilization using TCT as a facile linker, from which a novel DNA electrodechemical biosensor was constructed. Due to the surface area effect of GR and multi-site characteristic of CD in the composite, the surface density of the immobilized probe DNA on the biosensor was estimated as high as 3.82×10^{13} strands cm^{-2}. On the other hand, relying on the use of TCT as linker for DNA immobilization, the hybridization kinetic and efficiency of bioseneor are improved. Impedance-based hybridization assays show that the developed bioseneor demonstrated a low background response, an extremely high sensitivity for target DNA with a detection limit of 3.4×10^{-17} M, corresponding to 4.1×10^{3} molecules in 200 μL solution, indicating a promising application of the developed biosensor in real physiological sample without the help of the other amplification technology.

Acknowledgments

The work is supported by the National Natural Science Foundation of China (No. 21275127), Natural Science Foundation of Fujian Province (No. 2011J01059), Program for New Century Excellent Talents in Fujian Province University (No. JA12204).

References

Chen, X. Q., Wang, Q. X., Wang, L.H., Gao, F., Wang, W., Hu, Z. S., 2015. Biosens. Bioelectron. 66, 216-223.

Chen, Y., Wang, Q., Xu, J., Xiang, Y., Yuan, R., Chai, Y., 2013. Chem. Commun. 49, 2052-2054.

Cui, F., Zhang, X. L., 2012. J. Electroanal. Chem. 669, 35-41.

Cui, H. F., Xu, T. B., Sun, Y. L., Zhou, A. W., Cui, Y. H., Liu, W., John H. T. L., 2015. Anal. Chem. 87, 1358-1365.

Deng, J. H., Liu, M. L., Lin, F. B., Zhang, Y. Y., Liu, Y., Yao, S. Z., 2013. Anal. Chim. Acta 767, 59- 65.

Du, D., Zou, Z. X., Shin, Y. S., Wang, J., Wu, H., Engelhard, M. H., Liu, J., Aksay, I. A., Lin, Y. H., 2010. Anal.Chem. 82, 2989-2995.

Eck, M., Pham, C. V., Züfle, S., Neukom, M., Seßler,M., Scheunemann, D., Erdem, E., Weber, S., Borchert, H., Ruhstaller, B., Krüger, M., 2014. Phys. Chem. Chem. Phys. 16, 12251-12260.

Feng, L. Y., Zhang, Z. J., Ren, J. S., Qu, X. G., 2014. ACS Appl. Mater. Interfaces 6, 3513-3519.

Freeman, R., Finder, T., Bahshi, L., Willner, I., 2009. Nano Lett. 9, 2073-2076.

Guo, Y. J., Guo, S. J., Ren, J. T., Zhai, Y. M., Dong, S. J., Wang, E. K., 2010. ACS Nano 4, 4001-4010.

Keighley, S. D., Li, P., Estrela, P., Migliorato, P., 2008. Biosens. Bioelectron. 23, 1291-1297.

Li, X. L., Wang, X. R., Zhang, L., Lee, S., Dai, H. J., 2008. Science 319, 1229-1232.

Liu, Z. G., Zhang, A., Guo, Y. J., Dong, C., 2014. Biosens. Bioelectron. 58, 242-248.

Lu, L. M., Qiu, X. L., Zhang, X. B., Shen, G. L., Tan, W. H., Yu, R. Q., 2013. Biosens. Bioelectron. 45, 102-107.

Peng, Z. W., Lin, J., Ye, R. Q., Samuel, E. L. G., Tour. J. M., 2015. ACS Appl. Mater. Interfaces 7, 3414-3419.

Qin, Z., Taylor, M., Hwang, M., Bertoldi, K., Buehler, M. J., 2014. Nano Lett. 14, 6520-6525.

Rai, V., Nyine, Y. T., Hapuarachchi, H. C., Yap, H. M., Ng, L. C., Toh, C. S., 2012. Biosens. Bioelectron. 32, 133-140.

Shi, L., Chu, Z. Y., Dong, X. L., Jin, W. Q., Dempsey, E., 2013. Nanoscale

5,10219-10225.

Vickery, J. L., Patil, A. J., Mann, S., 2009. Adv. Mater. 21, 2180-2184.

Wang, Q., Ding, Y., Gao, F., Jiang, S., Zhang, B., Ni, J., Gao, F., 2013. Anal. Chim. Acta 788, 158-164.

Wang, X., Wang, Q., Wang, Q., Gao, F., Gao, F., Yang, Y., Guo, H., 2014. ACS Appl. Mater. Interfaces 6, 11573-11580.

Wang, Y., Li, Y., Tang, L., Lu, J., Li, J., 2009. Electrochem. Commun. 11, 889-892.

Wei, M. C., Tian, D., Liu, S., Zheng, X. L., Duan, S., Zhou, C. L., 2014. Sens. Actuators B 195, 452-458.

Whitaker, J. E., Haugland, R. P., Moore, P. L., Hewitt, P. C., Reese, M., 1991. Anal. Biochem. 198, 119-130.

Xia, H, Li, L. L., Yin, Z. Y., Hou, X. D., Zhu, J. J., 2015. ACS Appl. Mater. Interfaces. 7, 696-703.

Xu, Y. F., Liu, Z. B., Zhang, X. L., Wang, Y., Tian, J. G., Huang, Y., Ma, Y. F., Zhang, X. Y., Chen, Y. S., 2009. Adv. Mater. 21, 1275-1279.

Yang, C., Nakamura, A., Fukuhara, G., Origane, Y., Mori, T., Wada, T., Inoue, Y., 2006. J. Org. Chem. 71, 3126-3136.

Ye, X. L., Du, Y. L., Lu, D. B., Wang, C. M., 2013. Anal. Chim. Acta 779, 22-34.

Yu, L. H., Zheng, J. J., Xu, Y., Dai, D. X., He, S. L., 2014. ACS Nano 8, 11386-11393.

Zhang, J., Song, S. P., Zhang, L. Y., Wang, L. H., Wu, H. P., Pan, D., Fan, C. H., 2006. J. Am. Chem. Soc. 128, 8575-85809.

Zhang, Q., Zou, H. F., Wang, H. L., Ni, J. Y., 2000. J. Chromatogr. A 866, 173-181.

Zhang, S. S., Xia, J. P., Li, X. M., 2008. Anal. Chem. 80, 8382-8388.

Zhang, Z., Gu, S. Q., Ding, Y. P., Shen, M. J., Jiang, L., 2014. Biosens. Bioelectron. 57, 239-244.

Figure captions

Fig. 1. Diagram for the fabrication and hybridization procedures of the CD-GR based DNA biosensor.

Fig. 2. (A) Electronic photographs of GO (a), GR (b) and CD-GR (c) dispersions in water. (B) TEM image of CD-GR. (C) Raman spectra of GO (a), GR (b) and CD-GR (c). (D) FT-IR spectra of GR (a), CD (b) and CD-GR (c).

Fig. 3. Cyclic voltammograms (A) and Nyquist diagrams (B) of 1.0 mM $[Fe(CN)_6]^{3-/4-}$ (1:1) with 0.1 M KCl at bare GCE (a), CD/GCE (b), GR/GCE (c) and CD-GR/GCE (d). Inset shows the equivalent circuit diagram of the modified electrode.

Fig. 4. Chronocoulometric curves of 10 mM Tris-HCl (pH 8.0) without (a) and with (b) 50 μM RuHex at S1/TCT/CD-GR/GCE. Curve c is the chronocoulometric curve of 10 mM Tris-HCl (pH 8.0) with 50 μM RuHex at S1/TCT/CD-GR/GCE after hybridization with 1.0 nM S2.

Fig. 5. (A) Nyquist diagrams of 1.0 mM $[Fe(CN)_6]^{3-/4-}$ with 0.1 M KCl recorded at S1/TCT/CD-GR/GCE before (a) and after hybridization with 1.0×10^{-16} M (b), 5.0×10^{-16} M (c), 1.0×10^{-15} M (d), 5.0×10^{-15} M (e), 1.0×10^{-14} M (f), 5.0×10^{-14} M (g), 1.0×10^{-13} M (h), 1.0×10^{-12} M (i) complementary sequences (S2). (B) The plot of ΔR_{et} versus the logarithm of complementary sequences concentrations (lg C_{S2}). (C) Nyquist diagrams of 1.0 mM $[Fe(CN)_6]^{3-/4-}$ with 0.1 M KCl recorded on S1/TCT/CD-GR/GCE (a), S5-S1/TCT/CD-GR/GCE (b), S4-S1/TCT/CD-GR/GCE (c), S3-S1/TCT/CD-GR/GCE (d) and S2-S1/TCT/CD-GR/GCE (e), respectively. The concentrations for all the hybridized sequences are 1.0×10^{-14} M.

Highlights

- A water-soluble and stable CD-GR nanocomposite was synthesized through reduction method.
- CD-GR was used as an immobilization matrix for DNA for the first time.
- Due to the multi-site and surface area effects of CD-GR, the surface density was determined to be as high as 3.82×10^{13} molecules cm^{-2}.
- A wide linear range with low detection limit 3.4×10^{-17} M was achieved for the developed DNA biosensor.

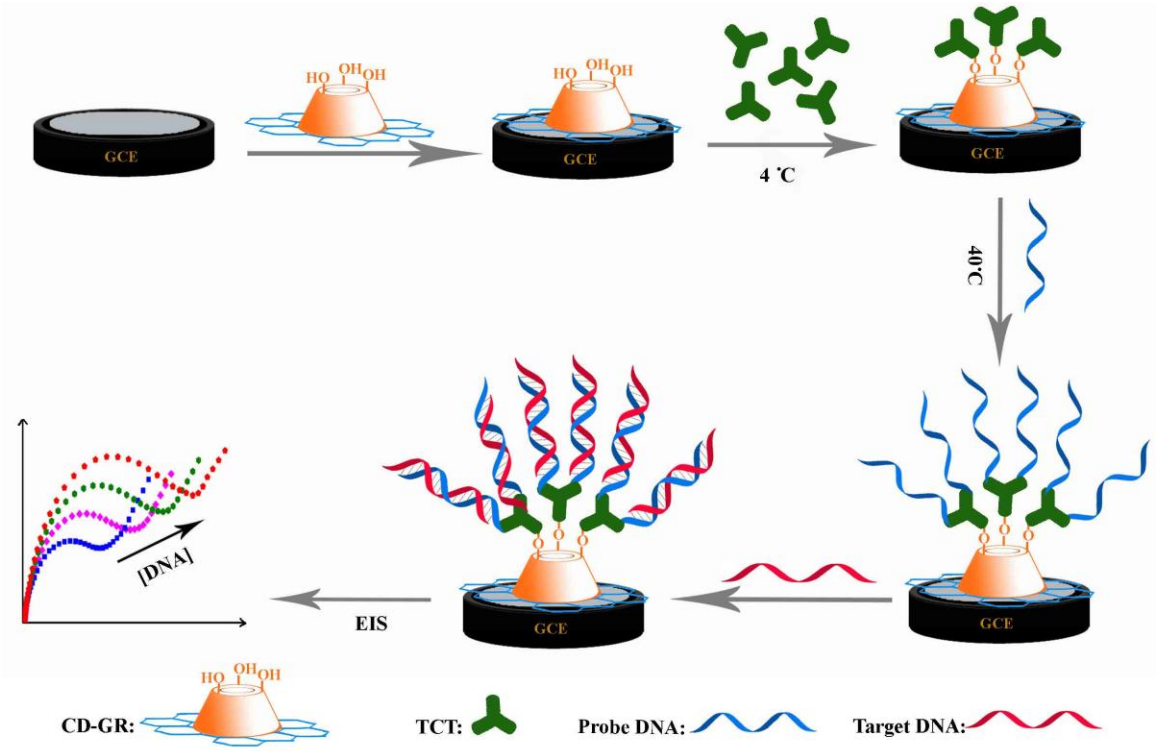
GCE
4 ℃
40 ℃
[DNA]
EIS
CD-GR:
TCT:
Probe DNA:
Target DNA:

Fig. 1

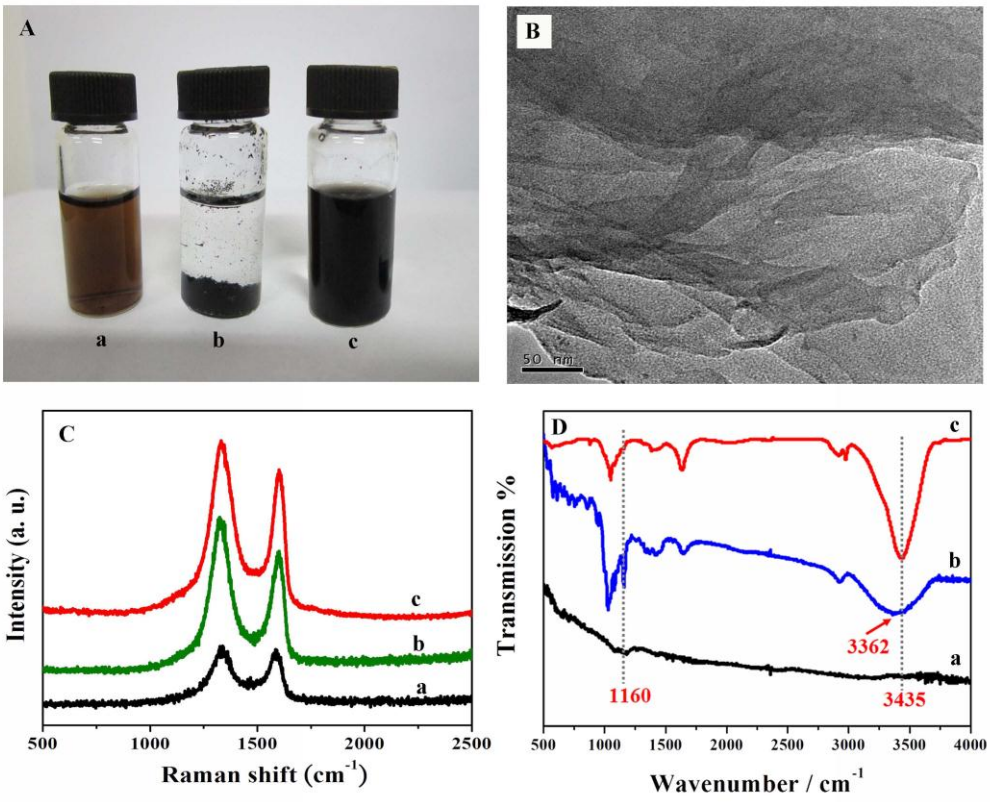
A
a
b
c
B
50 nm
C
Intensity (a. u.)
Raman shift (cm-1)
D
Transmission %
Wavenumber / cm-1
3362
1160
3435

Fig. 2

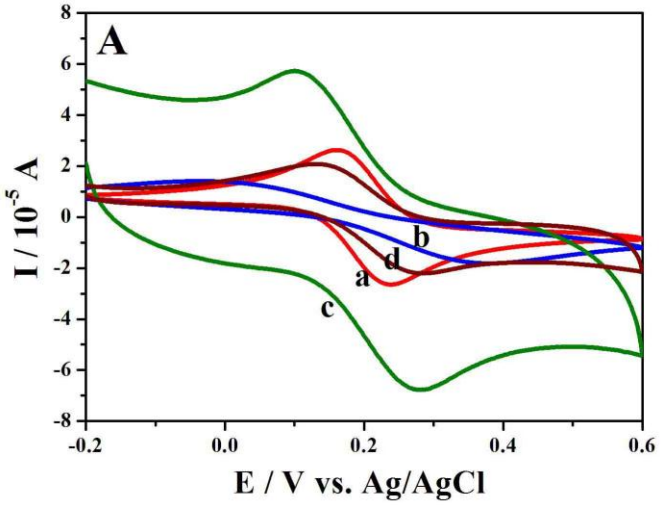
A
I / 10^-5 A
E / V vs. Ag/AgCl
a
b
c
d

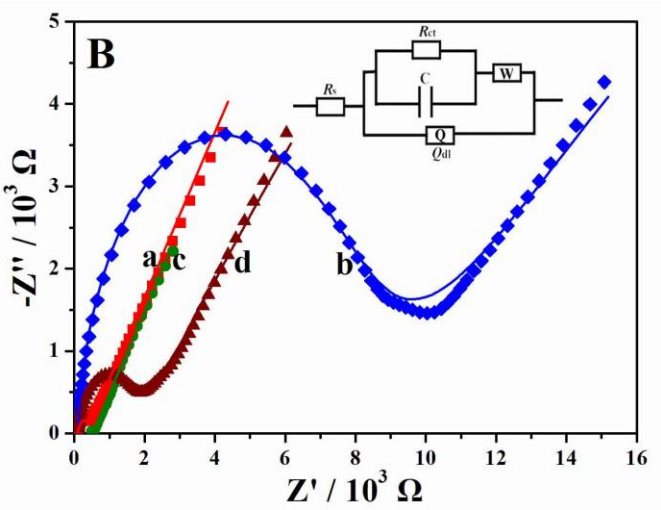
B
-Z'' / 10^3 Ω
Z' / 10^3 Ω
Rct
W
C
Rs
Q
Qdl
a
c
d
b

Fig. 3

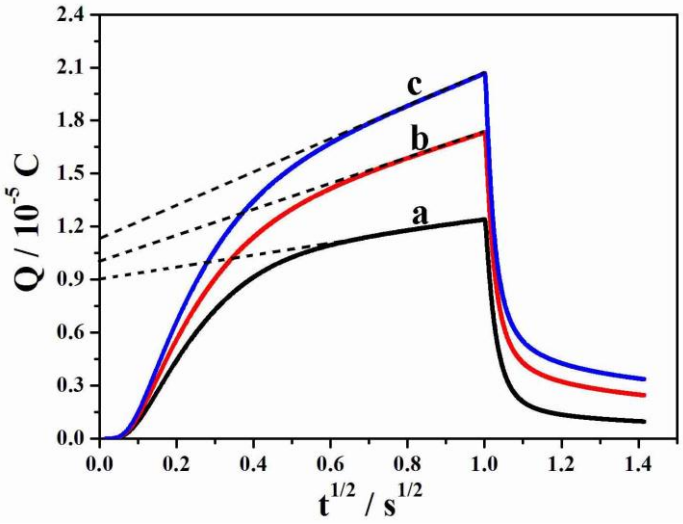
Q / 10^-5 C
t^1/2 / s^1/2
c
b
a

Fig. 4

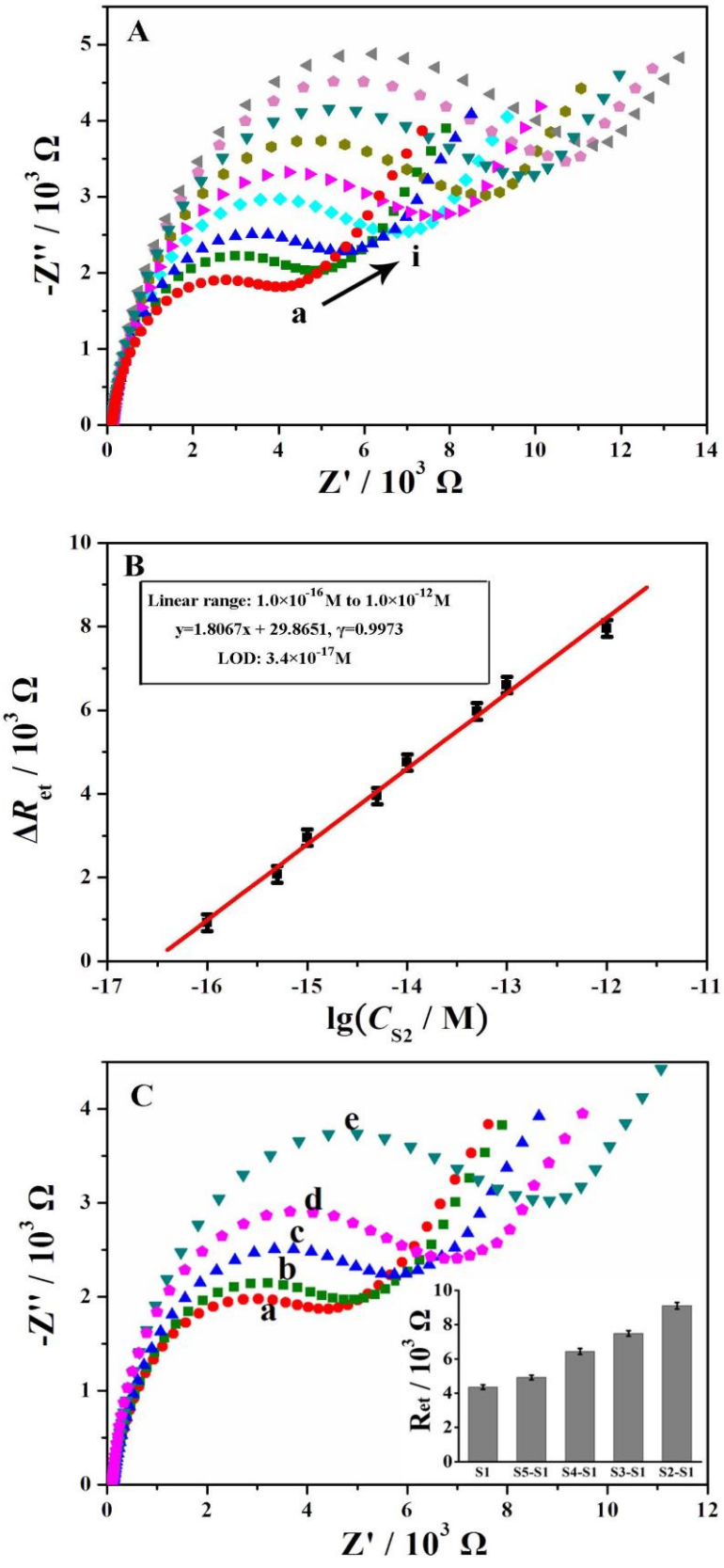
A
-Z'' / 10^3 Ω
Z' / 10^3 Ω
a
i
B
Linear range: 1.0×10^-16 M to 1.0×10^-12 M
y=1.8067x + 29.8651, γ=0.9973
LOD: 3.4×10^-17 M
ΔRet / 10^3 Ω
lg(CS2 / M)
C
-Z'' / 10^3 Ω
Z' / 10^3 Ω
a
b
c
d
e
Ret / 10^3 Ω
S1
S5-S1
S4-S1
S3-S1
S2-S1

Fig. 5